ELSEVIER

Journal of Electroanalytical Chemistry 379 (1994) 89–101

JOURNAL OF ELECTROANALYTICAL CHEMISTRY

Effect of axial ligands on the spectroelectrochemical properties of zinc phthalocyanine films. In situ Raman and electroreflection spectra

B.J. Palys [a,*], D.M.W. van den Ham [a], C. Otto [b]

[a] *Laboratory of Chemical Physics, University of Twente, 7500 AE Enschede, Netherlands*
[b] *Biophysical Technology Group, University of Twente, 7500 AE Enschede, Netherlands*

Received 30 July 1993; in revised form 30 March 1994

Abstract

Electroreflection and Raman spectra (in situ and ex situ) of zinc phthalocyanine (ZnPc) films (80 nm thick) have been studied. Raman spectra were resonantly and preresonantly enhanced. Both electroreflection and Raman experiments reveal the homogeneous inclusion of electrolyte anions upon oxidation of the film. The anions coordinate preferentially axial positions of the ZnPc molecule. This process is accompanied by an out-of-plane deformation of the phthalocyanine macrocycle, which results in the change of both electroreflection and Raman spectra. The ZnPc molecule remains deformed when the film is saturated with anions. The detailed analysis of new bands and altered intensities in the Raman spectrum indicates that the molecular symmetry point group changes from the D_{4h} point group to C_{2v}. The influence of ZnPc oxidation on the Raman excitation mechanism has been also studied. Effects of axial ligands on the molecular geometry have been studied by quantum chemical calculations for the $ZnPc^+$, $ZnPc^+Cl^-$ and $ZnPc^+(Cl^-)_2$ species using the unrestricted Hartree–Fock variant of the MNDO method. Calculation results show that the ZnPc molecule undergoes an out-of-plane deformation when one axial position is coordinated by the anion.

Keywords: Raman spectroscopy; Electroreflection spectroscopy

1. Introduction

Among various methods of chemical energy conversion to electricity, low-temperature fuels cells have received substantial interest (e.g. [1]). The main obstacle limiting their efficiency is the large overpotential which accompanies the cathodic reduction of molecular oxygen. Transition metal phthalocyanines (Pc) and naphthalocyanines (NPc) catalyse oxygen reduction with promising efficiency. However, both the activity and the stability of these catalysts are influenced by several factors.

Studies of iron phthalocyanine (FePc) and iron naphthalocyanine (FeNPc) monolayers adsorbed on various metal and carbon electrodes show that the type of the support partially determines the catalytic efficiency [2,3]: electron-donating groups present on the support surface enhance the catalytic activity [4]. It has been suggested, that these groups coordinate the phthalocyanine metal ion and via the change in the ligand field they influence the ability to bind molecular oxygen [5,6].

The axial coordination of the metal ion influences also the properties of FePc multilayer films (several hundred ångstroms thick). It has been observed that FePc films improve their catalytic activity during polarization at sufficiently cathodic potentials in the presence of oxygen. It has been proposed that oxygen enters the film and it is coordinated in the form of μ-oxo or μ-peroxo bridges [7].

From the above examples it follows that the coordination of Pc axial sites determines in part molecular properties. The understanding of this phenomenon is essential for optimizing the catalytic activity. This is also necessary to prevent the catalyst deactivation, observed for Pcs and NPCs (e.g. [8]). Catalyst stability is affected by both the support and the interaction with electrolyte anions: Coowar et al. [8] have shown that FeNPc impregnations on carbon black (from CH_4) are more stable in perchloric acid solution than in the sulphuric acid solution, while for the impregnations on

* Corresponding author.

SSDI 0022-0728(94)03490-T

Norit BRX carbon the reverse relation holds. The mechanism of the catalysts' deactivation has not yet been established. Some authors connect it with an oxidative attack on the Pc ligand [9–11], while others suggest rather the demetallation of phthalocyanine [12,13]. In this study we concentrated on the interaction of electrolyte anions with electrodes of chemical vapour deposited (CVD) zinc phthalocyanine (ZnPc) films.

ZnPc does not catalyse oxygen reduction, but its behaviour, upon anodic polarization, is the same as that observed for active iron and cobalt Pcs [14]. ZnPc has been chosen as a model compound because of its simple electrochemical properties: only the phthalocyanine ligand can be oxidized. Moreover, comparison with our previous spectroscopic studies of ZnPc [15,16] has been very useful in the interpretation of the present results.

If ZnPc films are conditioned by polarization at positive potentials, species from the electrolyte may enter the layer. Green and Faulkner [14] have shown that upon oxidation of ZnPc films in acid aqueous media, anions such as perchlorate and fluoride enter the film in order to maintain electroneutrality. A similar study of MgPc films has been published by Kahl et al. [17]. Both groups of authors have shown that the distribution of anions in these films is homogeneous. The intention of the present work was to check whether electrolyte anions are axially coordinated to the Pc metal centre and what the influence of axial coordination on Pc properties.

To follow the optical and chemical changes that are initiated by anodic oxidation of the ZnPc film, we used electroreflection (ER) and Raman spectroscopy. These methods yield complementary information about the intercalation of the electrolyte anions in the ZnPc film. In ER spectroscopy a sinusoidal voltage is superimposed on the dc electrode potential and changes in the reflected light intensity are detected. From this it follows that only that (small) part of the film that is oxidized and re-reduced contributes to the ER spectrum. A spectral change will occur when the optical properties of one or both of the redox components change. The method is sufficiently sensitive to detect electrochemical reactions with monolayers [7], hence the minute optical changes that are caused by the entry of ions into phthalocyanine multilayer films are large enough to permit the study of this effect with ER. In contrast to ER spectroscopy, the Raman method measures the scattered light of all the molecules that lie in the exciting laser beam. In the case of our thin ZnPc films, the whole film cross-section contributes and the resulting Raman spectrum can be a mixture of the spectra of reacted and unreacted parts of the film. We will show that it is plausible that changes in the Raman spectrum due to the interaction with ions can be attributed to changes in the molecular symmetry. We will discuss in detail effects of geometry changes on both Raman and ER spectra. The interpretation of changes in the Raman spectrum relies on the normal mode analysis we have performed previously [16]. The spectral data are compared with the results of quantum chemical calculations on the geometry of the $ZnPc^+$ ion (with and without axial ligands).

2. Experimental

The electrodes investigated were gold and glassy carbon discs covered with 80 mm thick ZnPc films. These films were deposited by the CVD method. The deposition rate was 0.05 nm s^{-1}. During deposition the film thickness was monitored by a quartz oscillator. These electrodes were used for both the Raman and the ER measurements. Prior to deposition the gold and glassy carbon discs were polished until mirror-like and rigorously cleaned by boiling in concentrated sulphuric acid followed by repeated boiling in Super-Q water. The counter electrode was a gold wire and the reference electrode an $Hg/HgSO_4$ electrode (MSE) (Radiometer K601). All potentials quoted are relative to this electrode (offset +620 mV vs. SHE). $HClO_4$, H_2SO_4 and benzenesulphonic acid solutions (pH = 1) were used as electrolytes. In some measurements H_2SO_4 and benzenesulphonic acid were mixed with $HClO_4$ (pH = 1). The modulation frequency was 30 Hz and the amplitude 30–50 mV. The ER apparatus has been described elsewhere [18]. In some measurements, a polarization filter was used. All ER spectra presented were measured at an incident angle of 25°.

Raman spectra were recorded either with a scanning double monochromator (Jobin-Yvon HGS) or a multichannel confocal Raman microspectrometer (CRM) [19,20]. The Raman spectra were obtained with 514.5 nm radiation from an argon ion laser or with 660 nm radiation from a dye laser (Spectra Physics Model 375B) operating with the 4-dicyanomethylene-2-methyl-6-[*p*-(dimethylamino)styryl]-4*H*-pyran (DCM) dye. The spectral resolution was 3 cm^{-1} for the scanning spectrometer and 6 cm^{-1} for the CRM. The times of recording the single spectrum were 20 min and 10 s, respectively. The electrochemical cell used in Raman measurements has been described previously [15].

3. Results

3.1. Electroreflection results

The ER results obtained with ZnPc films deposited on gold and on glassy carbon supports are very much alike and so only the ER and Raman results for ZnPc films on glassy carbon are presented.

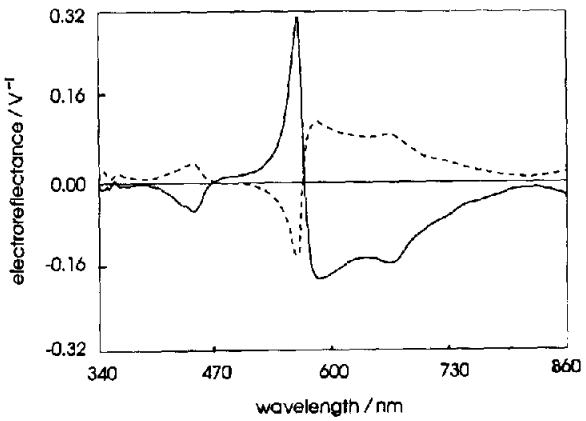

Fig. 1. ER spectra of the ZnPc film at +100 mV (OCP): ac frequency, 30 Hz; ac amplitude, 30 mV; supporting electrolyte, 0.1 M $HClO_4$. Solid line, in-phase (real) signal; dashed line, out-of-phase (imaginary) signal.

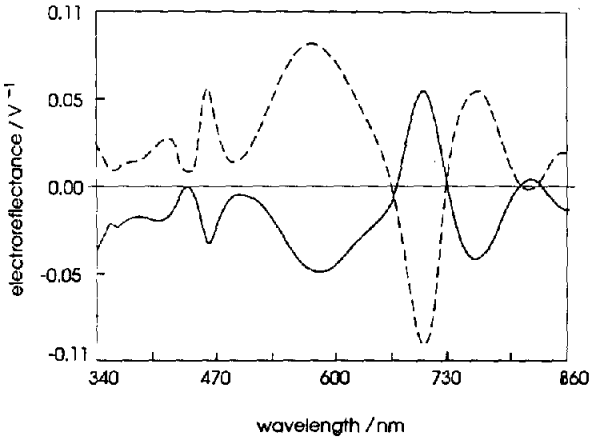

Fig. 3. ER spectra of the ZnPc film at +300 mV: ac frequency, 30 Hz; ac amplitude, 30 mV; supporting electrolyte, 0.1 M $HClO_4$. Solid line, real signal; dashed line, imaginary signal.

Figs. 1–8 show the ER spectra of the same ZnPc film deposited on a glassy carbon substrate but measured sequentially one after another. In these measurements 0.1 M $HClO_4$ solution was used as the electrolyte. Although it is customary to present only the in-phase part of the ER signal, we present here out-of-phase part as well (see Discussion).

Fig. 1 shows the ER spectrum of a freshly prepared ZnPc film measured at a dc potential of +100 mV (vs. MSE). This potential is 30 mV more positive than the open circuit potential (OCP). The spectrum does not change with time at this bias. The spectrum in Fig. 2 was measured after the former but at a larger bias (+200 mV), the only difference being the spectral amplitude. The recording of an ER spectrum over a 500 nm wavelength range takes about 1 h.

The spectra in Figs. 3, 4 and 5 were each measured at a dc potential of +300 mV. These spectra differ in shape. Fig. 6 was recorded at +100 mV after being kept at +300 mV overnight. The spectrum in Fig. 7 was measured at +100 mV after keeping the film for 14 h at −100 mV. The spectrum in Fig. 8 was also measured at +100 mV, but the electrode was taken out of the cell and dried under vacuum for 24 h prior to the measurement.

In Figs. 4 and 5 two boxes have been drawn. Their function is to draw the attention to the fact that at this wavelength the two spectral components (see Discussion) do not become zero simultaneously. This observation was further investigated by recording a series of short-wavelength scans (650–750 nm) at a potential of +300 mV on a fresh ZnPc electrode. This short range was chosen because the time span it takes to measure a spectrum (ca. 10 min) permitted the observation of the evolution of that part of the spectrum in small steps. Apart from the moment of measurement, the spectra differed in the fact that they were recorded with unpolarized, *s*-polarized or *p*-polarized light (Fig. 9(a)–(h)). The real and imaginary components of the spectrum become zero simultaneously only in the *s*-polarized spectra.

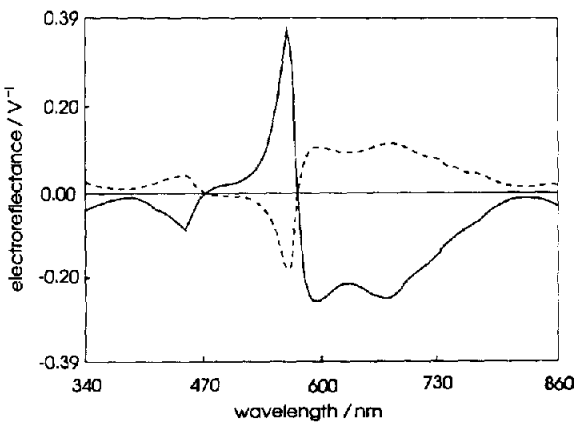

Fig. 2. ER spectra of the ZnPc film at +200 mV: ac frequency, 30 Hz; ac amplitude, 30 mV; supporting electrolyte, 0.1 M $HClO_4$. Solid line, real signal; dashed line, imaginary signal.

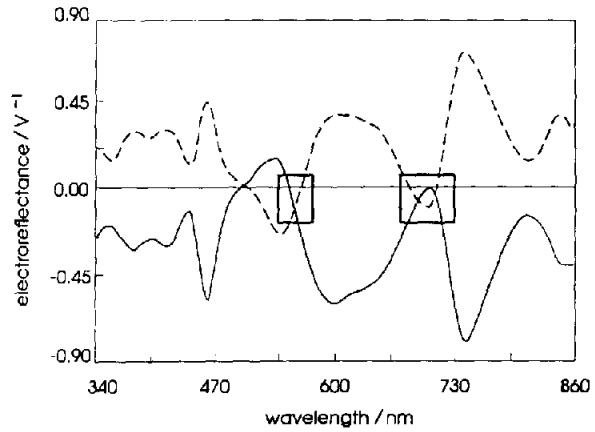

Fig. 4. ER spectra of the ZnPc film at +300 mV: ac frequency, 30 Hz; ac amplitude, 30 mV; supporting electrolyte, 0.1 M $HClO_4$. Solid line, real signal; dashed line, imaginary signal.

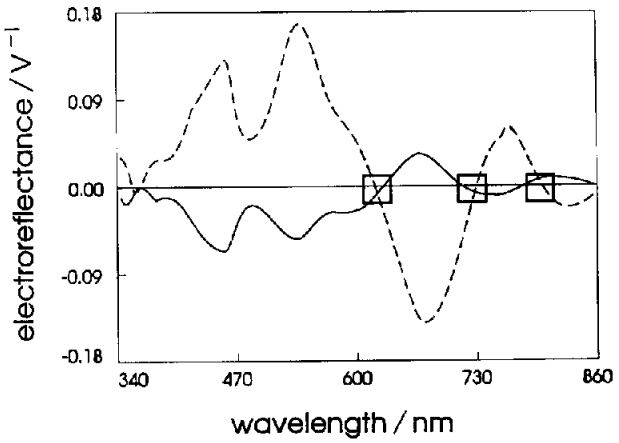

Fig. 5. ER spectra of the ZnPc film at +300 mV: ac frequency, 30 Hz; ac amplitude, 30 mV; supporting electrolyte, 0.1 M $HClO_4$. Solid line, real signal; dashed line, imaginary signal.

ER spectra measured up to +300 mV in sulphuric and benzenesulphonic solutions are identical with those in Figs. 1 and 2. Above this potential the ZnPc film breaks down. Addition of a small amount of perchlorate anions to the sulphuric acid solution causes changes in the spectrum (at +300 mV) similar to those observed in the pure $HClO_4$ electrolyte. Addition of perchlorate to the benzenesulphonic acid solution does not have any effect.

3.2. Raman results

The Raman spectra presented in this section were obtained with lasers operating either at 514.5 nm (green) or at 660 nm (red). The spectra were recorded under experimental conditions that are comparable to the conditions under which the ER spectra were measured, i.e. the ZnPc film was polarized at the OCP and at more positive potentials where the oxidation of the

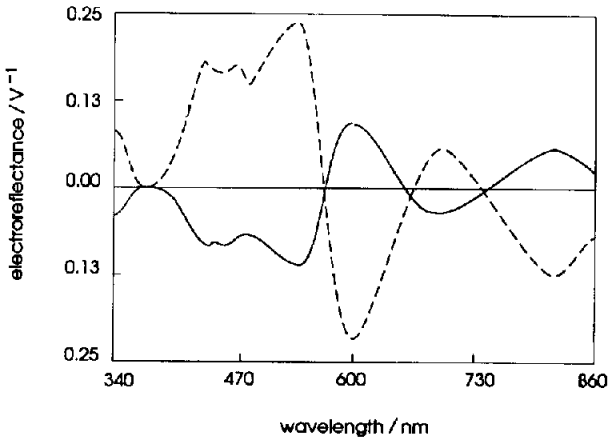

Fig. 6. ER spectra of the ZnPc film at +100 mV after one night at +300 mV: ac frequency, 30 Hz; ac amplitude, 30 mV; supporting electrolyte, 0.1 M $HClO_4$. Solid line, real signal; dashed line, imaginary signal.

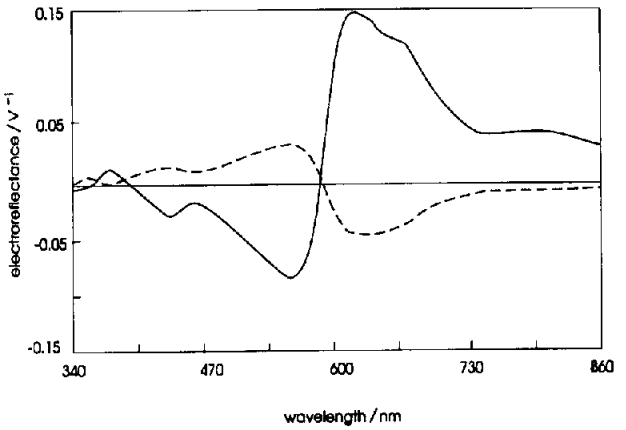

Fig. 7. ER spectra of the ZnPc film at +100 mV after 14 h at −100 mV: ac frequency, 30 Hz; ac amplitude, 30 mV; supporting electrolyte, 0.1 M $HClO_4$. Solid line, real signal; dashed line, imaginary signal.

film takes place. Comparison of the Raman and ER results is therefore meaningful. Fig. 10(a)–(e) show spectra recorded with 660 nm laser radiation: (a) is the spectrum of the original ZnPc layer on glassy carbon at the OCP of +70 mV, and must be compared with the ER spectrum in Fig. 1; (b) is the spectrum resulting after polarization of the film at 250 mV and corresponds to the ER picture in Fig. 2; (c) and (d) spectra occur during polarization at 350 mV and should be compared with the ER spectra in Figs. 5–7; spectrum (e) does not change with prolonged polarization periods and has to be compared with the ER spectrum in Fig. 6; spectrum (f) results after keeping the electrode at a negative potential (−50 mV) of the original OCP. Spectrum (f) is similar to the original one (a), but it is not exactly the same; it should be compared with the ER spectrum in Fig. 7.

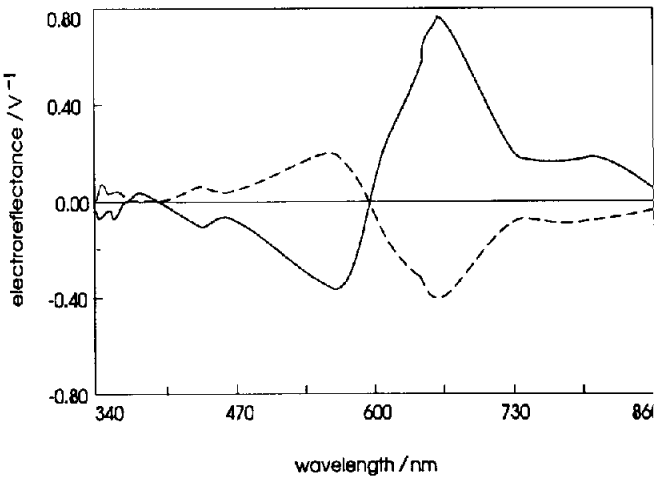

Fig. 8. ER spectra of the ZnPc film at +100 mV after 15 h under vacuum: ac frequency, 30 Hz; ac amplitude, 30 mV; supporting electrolyte, 0.1 M $HClO_4$. Solid line, real signal; dashed line, imaginary signal.

The spectra in Fig. 11(a) and (b) were recorded ex situ with 514.5 nm laser radiation. The former spectrum is that of neutral ZnPc and the latter is that of the oxidized form and should be compared with the ER spectrum in Fig. 6.

3.3. Calculations on the oxidized ZnPc molecular structure

During the anodic polarization of the ZnPc film the phthalocyanine molecules are oxidized to $ZnPc^+$ ions

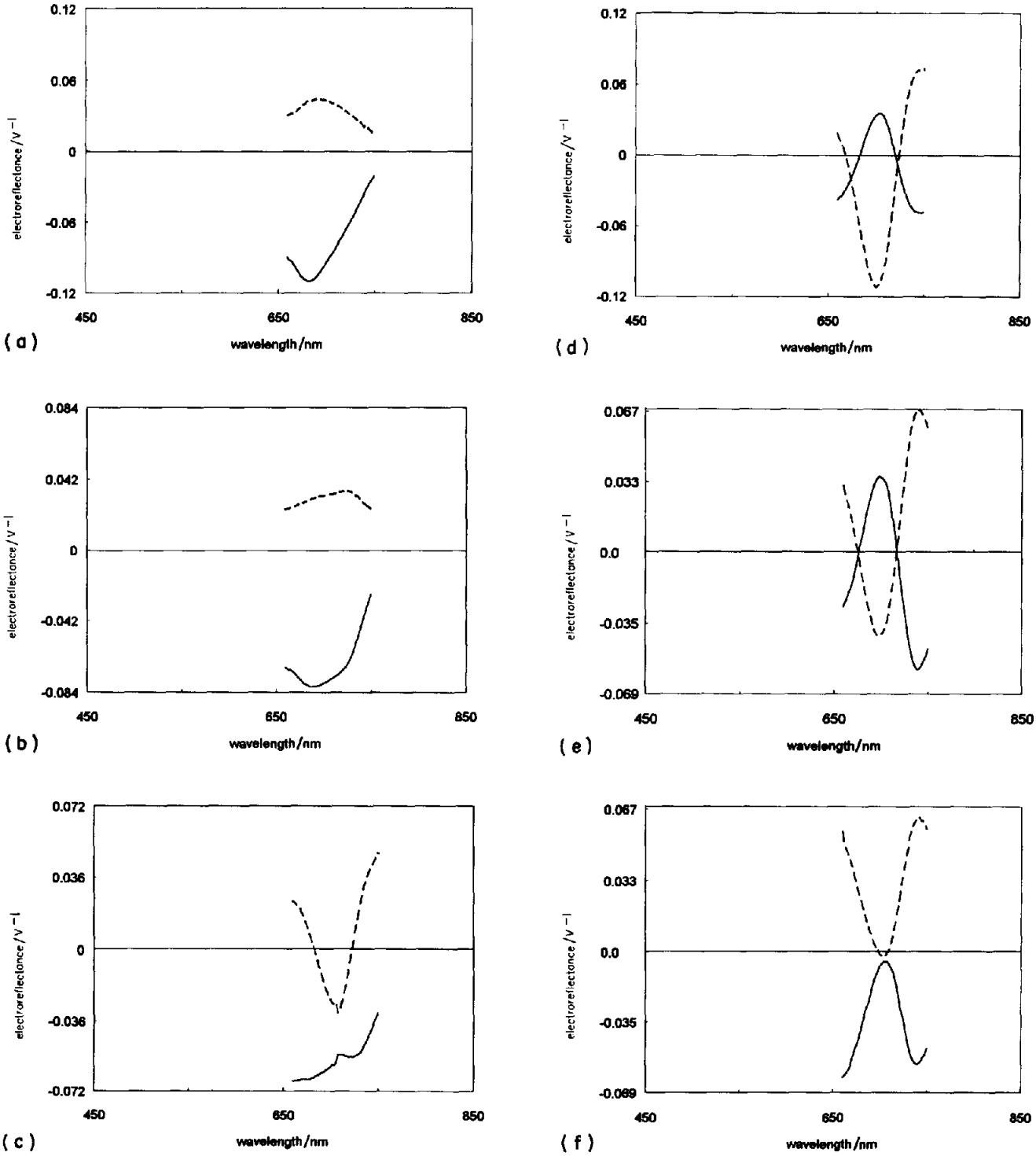

Fig. 9. ER spectra of the ZnPc film. (a)–(h) Series of successive scans at +300 mV recorded with *s*- and *p*-polarized and unpolarized light; ac frequency, 30 Hz; ac amplitude, 30 mV; supporting electrolyte, 0.1 M $HClO_4$. Solid line, real signal; dashed line, imaginary signal.

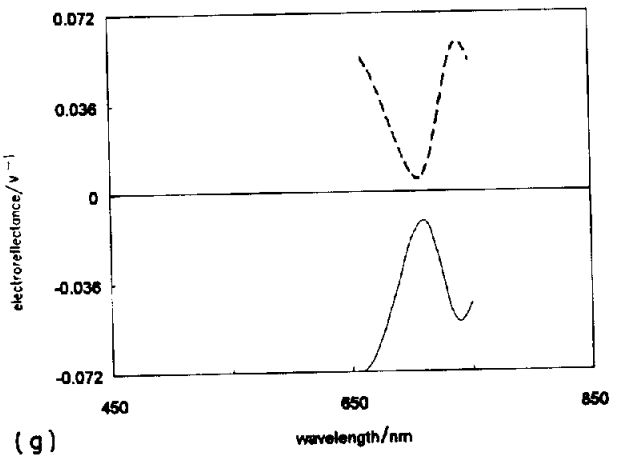

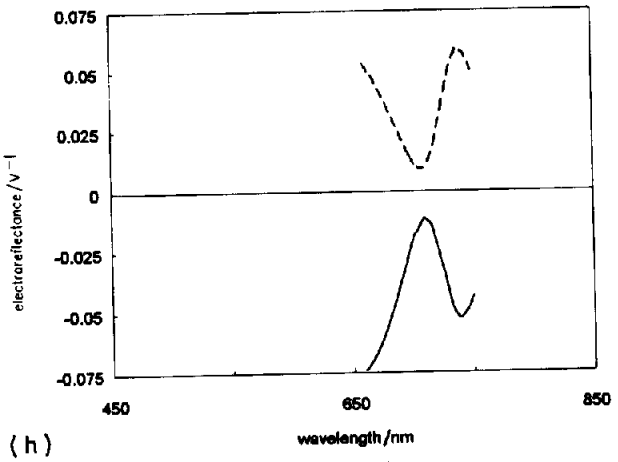

Fig. 9 (continued).

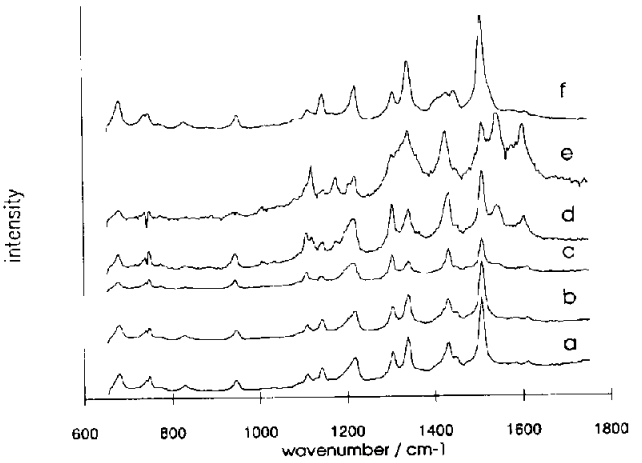

Fig. 10. Raman spectra (excitation with 660 nm radiation) of the ZnPc film recorded, (a) at OCP (70 mV) potential; (b) at 250 mV potential; (c) after ca. 7 min of polarization of the electrode at 350 mV; (d) after ca. 40 min of polarization of the electrode at 350 mV; (e) stable spectrum after ca. 2 h of polarization at 350 mV; (f) rereduced layer after ca. 5 min at a potential of −100 mV.

[14]. In order to study the influence of both the change of the oxidation state and the interaction with the electrolyte anions we calculated the geometries of $ZnPc^+$ ion, the $ZnPc^+$ complex with the chlorine ($ZnPc^+Cl^-$) and the complex with two chloride anions ($ZnPc^+(Cl^-)_2$ negative ion). The chloride anions were used instead of perchlorate anions to simplify the calculation. Since $ZnPc^+$ has an odd number of electrons, the unrestricted Hartree–Fock (UHF) variant of the MNDO method was applied. To keep the results comparable with those for neutral ZnPc, we applied the UHF/MNDO method also for the ZnPc molecule.

Calculations were performed with the aid of the VAMP program [21] run on a Convex computer. The optimized geometries are presented in Fig. 12. Table 1 summarizes the zinc–nitrogen bond distances and angles.

Both the ZnPc molecule and the $ZnPc^+$ ion (Fig. 12(a)) are flat and belong to the D_{4h} molecular point group. Differences in the Zn–N bond lengths increase through both the oxidation and the attachment of the chloride anions to the zinc centre.

Bonding of the single chloride anion to the zinc centre causes the out-of-plane deformation of the whole phthalocyanine macrocycle (Fig. 12(b) and Table 1). When two chloride anions are placed on the opposite

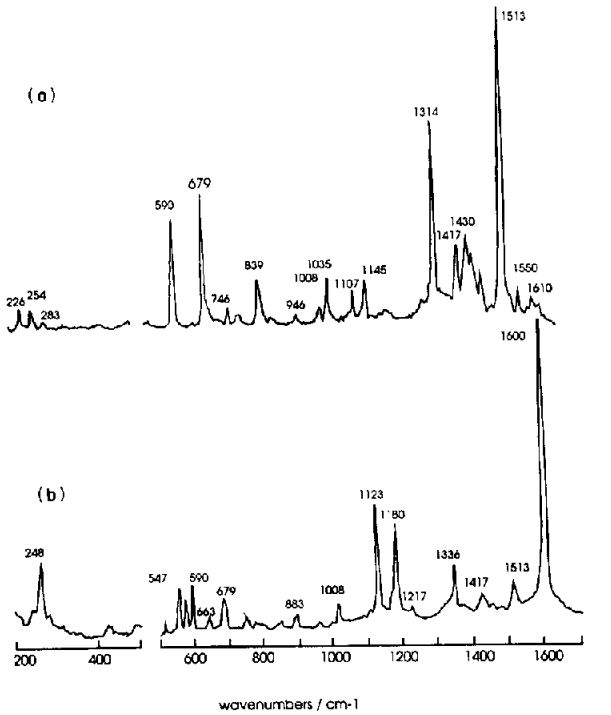

Fig. 11. Ex situ Raman spectra (514.5 nm excitation) of the ZnP film: (a) electrochemically untreated film; (b) film after ca. 2 h o anodic polarization at +350 mV.

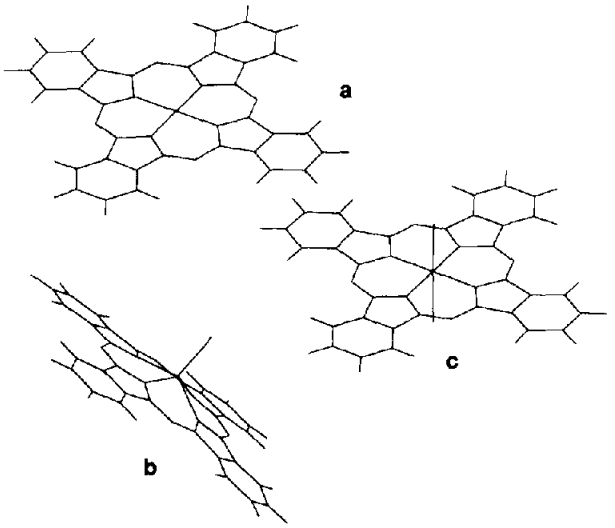

Fig. 12. Optimized geometries of ZnPc molecule: (a) $ZnPc^-$; (b) $ZnPc^+ Cl^-$; (c) $ZnPc^+(Cl^-)_2$.

sides of the $ZnPc^-$ ion, the calculated structure become flat again (Fig. 12(c)).

4. Discussion

4.1. Electroreflection and calculation results

In ER measurements a sinusoidally modulated voltage is superimposed on a dc electrode potential. The dc potential is to ensure that both redox components of the ZnPc film are present. The ac voltage changes the ratio between those forms. If these have different optical spectra, the light reflected from the electrode surface will change with the same frequency as the applied ac voltage. This change is analysed with a lock-in amplifier for all wavelengths and the result, the ER spectrum, is usually displayed as either the real and/or the imaginary component of the lock-in amplifier output versus the wavelength. When the optical properties of both redox forms happen to be equal at some wavelength, the ac voltage does not change the reflectivity and consequently the ER signal must be zero at this wavelength. From the ratio of the real and imaginary parts of the spectrum the phase angle can be calculated. A phase angle that is constant in time means that no chemical or physical reactions follow the electrochemical step.

Such a situation occurs in the ER spectrum in Fig. 1, so at this dc potential the only reaction taking place is the redox reaction $ZnPc \rightarrow ZnPc^+$ and vice versa. This is still the case at a bias of +200 mV. At higher potentials the ER spectra begin to change in form and in phase angle (Figs. 3–5). The explanation for this change is that when the potential is made more positive, an increasing part of the film becomes oxidized and so positively charged. This accumulation of charge in the film cannot go on and is either compensated for by the uptake of ions from the electrolyte or by destruction of the film. Green and Faulkner [14] studied this effect with a number of Pc films, among them films of ZnPc. They found that the oxidation followed by incorporation of anions is essentially reversible, i.e. on reduction the anions are expelled. In the model of these authors, the anions enter and depart along the grain boundaries of the grains that form the film. The anions are homogeneously distributed. This followed from Auger depth profiles that were flat from the surface of the film to its boundary with the support [14]. In the electrochemical experiments of Green and Faulkner [14] the potential was stepped between 0 and 1 V vs. SCE (ca. −400 to 600 mV vs. MSE). In the experiments presented here the highest potential was +300 mV. This potential difference explains why total oxidation of the film took hours in the experiments presented here compared with seconds in the experiments of Green and Faulkner [14].

On the basis of results of Green and Faulkner [14] and Kahl et al. [17], it is reasonable to assume here that changes in the ER spectra in Figs. 3–5 are the result of the uptake of perchlorate anions by the film. After a certain period at +300 mV the film is completely oxidized and saturated with anions. When this situation is obtained, the ER spectrum stops changing. This is indeed the case and the ER spectrum in Fig. 6 is typical for the steady-state situation at a potential of +300 mV. When the "saturated" film is kept at a sufficiently negative potential, the film is rereduced and the anions are expelled. The resulting ER spectrum (Fig. 7), measured at +100 mV, differs, however, from Fig. 1. To exclude the possibility that this difference is due to the presence of water in the layer, the electrode was removed from the cell and dried in vacuum. After remounting the electrode, the ER spectrum in Fig. 8 was obtained. It still differs from that in Fig. 1. The conclusion must be that uptake and expul-

Table 1
The calculated zinc–nitrogen bond distances and angles

Coordinate	ZnPc	$ZnPc^+$	$ZnPc^+Cl^-$	$ZnPc^+(Cl^-)_2$
$Zn-N_2$ Å	2.0191	2.0177	2.0121	2.0538
$Zn-N_3$ Å	2.0190	2.0296	2.1565	2.0860
$Zn-N_4$ Å	2.0192	2.0302	2.1575	2.0860
$Zn-N_5$ Å	2.0189	2.0173	2.1214	2.0541
N_3-Zn-N_2 °	90.472	89.856	83.978	90.068
N_4-Zn-N_3 °	89.522	89.785	84.246	89.306
N_5-Zn-N_4 °	90.474	90.589	83.902	90.067
N_5-Zn-N_2 °	89.533	89.771	84.247	90.088
Zn out-of-plane deformation by atoms: N_2, N_3, N_4 Å	0.0000	0.0001	0.6930	0.0100

sion of the perchlorate anions change the structure of the film. So far, these results confirm those of Green and Faulkner [14].

Repetition of the experiments in 0.05 M sulphuric acid showed that up to +300 mV the ER spectrum remains as in 1 and 2. Above this potential the film breaks down. Addition of a small amount of perchlorate anions to the (sulphuric acid) electrolyte immediately causes the ER spectrum to change in the way described above for the case of the perchloric acid electrolyte. It seems as if perchlorate anions can enter the film whereas the sulphate anions cannot. It is hard to imagine that ion transport along grain boundaries proceeds easily in the case of perchlorate anions but is impossible in the case of the sulphate anion. The explanation is that although the sulphate anions enter the film along grain boundaries, they cannot, in contrast to the perchlorate anions, enter the grains. The reason for this difference is the size of the sulphate anion due to its hydration shell. The competition experiment was repeated with a benzenesulphonic acid solution as the electrolyte. Addition of perchlorate anions did not alter the spectral shape. Here the large benzenesulphonic acid molecules also impede access of perchlorate anions to the grains.

In the spectra in Figs. 4 and 5 the boxes emphasize unexpected ER behaviour, that is, the ER signal changes rapidly from pure real to imaginary or vice versa. Although this effect is normal for the spectral range where the (halogen) lamp's light intensity is low (UV side) or the photomultiplier sensitivity diminishes (IR side), it is not likely that limitations in the apparatus are responsible for this ER behaviour in the 650–750 nm range. Moreover, the effect is observed only during the period that the perchlorate anions migrate through the film. The series of spectra in Fig. 9 show that the effect reveals itself only in the *p*-polarized component of the incident light. The fact that the intensities of the spectra with *p*- and *s*-polarized light are about equal excludes an explanation in terms of apparatus instability. The other explanation is that two processes occur, each with its own phase angle. In the following discussion it is assumed that the majority of the ZnPc molecules in the film have their molecular plane parallel to the electrode surface (the order and the orientation of molecules in the phthalocyanine film depend on the deposition rate [22]; in the films we used (deposition rate 0.05 nm s^{-1}) the molecules are well ordered and the orientation parallel to the supporting surface is the most probable one). From this assumption it follows that the electric vector of *s*-polarized light is always parallel to the ZnPc molecular plane while the electric vector of *p*-polarized light has both parallel and perpendicular components. Consequently a reorientation of ZnPc molecules in the film can change the shape and intensities of *s*- and *p*-polarized spectra, but it cannot be the reason for the lack of simultaneous zero crossings of the real and imaginary components of the ER spectrum. For the explanation of the latter effect one must realize that at measured wavelength region (around 700 nm) the optical properties of ZnPc and of its reduced form are determined by electronic transitions from HOMO to LUMO. The ZnPc molecule has D_{4h} symmetry, and these MOs belong respectively to the a_{1u} and e_g representation. Transitions between these MOs are x,y allowed and forbidden in the z direction.

As a consequence, *s*-polarized light (parallel to the molecular plane) can cause only electronic transitions in the x and y directions while *p*-polarized light can, in principle, cause transitions in the z direction too. The latter transitions are forbidden in ZnPc for symmetry reasons. If, however, a situation arises in which the Zn ion is forced out of the molecular plane, this interdiction is no longer valid. This situation will arise when anions enter the ZnPc film and locate themselves in axial positions. The calculations (see Results) show that out-of-plane distortions of the $ZnPc^+$ ion can easily exceed 0.05 nm when oxidation of ZnPc is combined with the presence of an anion on the one axial position.

This distortion is a process that follows the electrochemical step and as a consequence electronic transitions in the z direction have a different phase difference with the modulating voltage than the transitions in the x and y directions.

After complete oxidation of the film, the transient behaviour is no longer observed. Two possible conclusions can be drawn from this observation: (1) the transition in the z direction becomes forbidden again or (2) the process that gives rise to the transition in the z direction no longer has a phase angle that differs from that of the transitions in the x and y directions. The former case can arise when both axial positions of the ZnPc molecule are occupied by ClO_4^- anions and that every ClO_4^- ion is bound to two ZnPc molecules (see Fig. 13(a)). On the basis of calculation results it can be assumed that in this situation the molecule becomes planar again. The fact that the measured

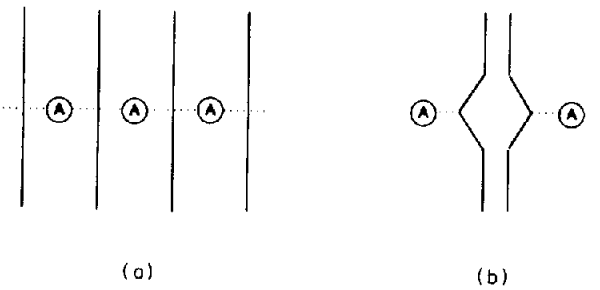

Fig. 13. Two possible structures of the ZnPc film saturated with electrolyte anions. A = anions.

ClO_4^-/ZnPc ratio is unity at this stage of oxidation [14] agrees with this explanation. The second possibility arises when oxidized and reduced forms of the molecules in the film are both non-planar. Then the distortion no longer follows the electrochemical step and no extra phase angle appears. For this latter explanation too there is experimental evidence. Myers et al. [23] have measured that ZnPcCl is diamagnetic. Since this molecule contains an odd number of electrons, this diamagnetism must arise through spin pairing. These authors suggest the formation of dimers in which two five-coordinate ZnPcCl units are stacked with their phthalocyanine bases parallel and with electron coupling through the π clouds (see Fig. 13(b)). It seems reasonable that similar structures are formed after intercalation of ClO_4^- anions. Such units in which the central Zn ion is five-coordinated are not planar according to calculation results.

Finally, on the basis of the ER data it can be concluded that upon oxidation (some of) the ZnPc molecules become distorted, at least temporarily. However, ER spectroscopy cannot discern between the two possible final forms of the layer.

4.2. Raman spectra

In an attempt to make a choice between two possible structures of the ZnPc film, Raman spectra were measured inside and outside the electrochemical cell.

The Raman spectrum in Fig. 10(b) (potential +250 mV) does not differ from that of the original neutral film (Fig. 10(a)). This observation is in agreement with the steady state observed for the ER spectra at this potential. The spectra in Fig. 10(c) and (d) were measured at a polarizing potential of +350 mV. These spectra change with time and hence should be compared with the transient period of the ER experiments. After 2 h no further changes occur (Fig. 10(e)) and there are no differences between the Raman spectra recorded in situ and ex situ. The latter observation means that the observed changes are due to changes in the film alone and are not a simple effect of the applied potential (electric field effect). Re-reduction of the film (Fig. 10(b)) yields exactly the spectrum of the original neutral form, so the intercalation process is reversible. This observation is in agreement with the ER results and those of Faulkner and co-workers [14,17]. Slight differences in the region of 1400 cm^{-1} are possibly caused by the altered layer structure.

Care must be taken in the comparison of ER and Raman spectroscopic results. Because the Raman spectrum reflects the averaged spectral properties of the oxidized and reduced forms of the film it is not in contradiction to the ER results that the Raman spectrum keeps changing during the entire oxidation period.

The spectrum in Fig. 10(e) corresponds to the ZnPc film saturated with anions. Differences between this spectrum and that of the neutral ZnPc film (Fig. 10(a)) are very pronounced: new bands and altered relative intensities are observed. Since Raman selection rules depend on the molecular symmetry, this type of change indicates an altered molecular geometry. In the case of ZnPc also the change of the Raman excitation mechanism must be considered: oxidation of the ZnPc molecule shifts significantly (ca. 150 nm) the Q absorption band towards shorter wavelengths [14,24]. Such a shift must alter the Raman spectrum. To be sure that this shift is not the only factor causing changes in the Raman spectrum, we applied two excitation lines: the spectra in Fig. 10 were recorded using 660 nm radiation (red) and those in Fig. 11 using 514.5 nm radiation (green). The wavelength of the red radiation coincides with the maximum of the Q band of neutral ZnPc but lies on the long wavelength shoulder of the oxidized form. Therefore, the Raman spectrum of neutral ZnPc excited with red radiation is resonance enhanced (Fig. 10(a) and (f)) whereas the spectrum of oxidized form is preresonance enhanced (Fig. 10(b)–(d)). The preresonance enhanced spectra are about 10 times less intense than the resonance enhanced spectra. The green radiation coincides with the short-wavelength side of the Q band of the oxidized form but coincides only with the short-wavelength tail of the Q band of the neutral form. The spectra of both forms can be considered as preresonance enhanced spectra. The spectra of the neutral form excited by green radiation are less intense by a factor 15, thus reflecting its larger deviation from the resonant situation.

The same kind of change is observed in both spectra excited with red and green radiation. This makes it more likely that the observed spectral changes do not result only from the change in the excitation mechanism. This conclusion agrees with resonance Raman studies of ZnPc monolayers. In the case of monolayer spectra the oxidation of the layer caused only a change of Raman intensity [15] and the band positions were not shifted significantly. In particular, the strong band at 1600 cm^{-1} (Figs. 11(b) and 10(e)) was not observed. Consequently, we may conclude that the changes we observe in the Raman spectra of ZnPc films are not exclusively the consequence of the oxidation of the ZnPc molecule. We are obliged to consider the change of the molecular geometry as well. We can conclude further that the change of the molecular geometry is possibly caused by an interaction with electrolyte anions entering the layer.

The possible change of the molecular geometry allows us to explain the most significant spectral change, the appearance of new bands at 547, 567, 633, 883 and 1600 cm^{-1}. It might be possible that the strong band at 1600 cm^{-1} originates from the shift of the 1513 cm^{-1}

band, although such a shift is very large. It would be surprising that other bands do not shift so significantly. Moreover, the decrease of the 1513 cm^{-1} band and the increase of the 1600 cm^{-1} band are dependent on the excitation line. It is more pronounced in the spectrum excited by 514.5 nm radiation than in the spectrum excited by the 660 nm radiation (compare Figs. 10(e) and 11(b)). For these reasons we assume that the 1600 cm^{-1} band is the new band appearing after the oxidation rather than the shifted 1513 cm^{-1} band.

The analysis of new bands appearing after oxidation of the ZnPc film gives information about the form of this distortion. Further it enables one to choose between two possible structures of the oxidized film, which have been proposed on the basis of electroreflection and calculation results (Fig. 13(a) and (b)). To perform such analysis one has to consider changes of Raman selection rules caused by possible molecular distortions.

When the excitation line lies far from the absorption maximum, the Raman-active modes have the same symmetry as the elements of the polarizability tensor. Using the group table [25] we find that for the ZnPc molecule (D_{4h}) they are A_{1g}, B_{1g}, B_{2g} and E_g vibrations in the normal Raman spectrum. In the resonance Raman effect two types of enhancement occur [26,27]. The A-type enhancement operates for totally symmetric vibrations (A_{1g} for D_{4h} group). The B-type enhancement allows modes having symmetries that are contained in the direct product representation of the two electronic transitions that contribute to the resonance enhancement. In the case of phthalocyanines these are the Q and Soret bands. These transitions both have E_u symmetry if the molecular symmetry is D_{4h}. The direct product $(E_u \times E_u)$ contains the A_{1g}, A_{2g}, B_{1g} and B_{2g} representations, and therefore modes with these symmetries are enhanced. Studies of resonance Raman spectra of phthalocyanines and porphyrins [28–30] show that the B-term scattering is very strong in spectra excited in the Q-band region. We assume that ZnPc spectra show similar characteristics and B-term scattering is effective in spectra excited in resonance with the Q absorption band.

The above consideration shows that if we pass from the resonance to the normal Raman spectrum we expect a decrease of A_{2g} bands and growth of E_g bands relative to the bands of species A_{1g}, B_{1g} and B_{2g}. From the experimental results it follows that the changes in the Raman spectrum caused by the oxidation of the ZnPc film are more significant. Therefore, we are obliged to consider also possible effects of the molecule deformation on the Raman spectrum. The out-of-plane deformation of the ZnPc molecule involves a change of the molecular point group from D_{4h} to C_{4v} or C_{2v} and the in-plane deformation results in C_s symmetry. By considering different symmetry elements of these point groups we can find how the ZnPc vibrations transform in lower symmetry groups. For example, B_{1g} vibrations are not symmetric with respect to the main (fourfold) symmetry axis and they are symmetric with respect to the vertical plane and to the symmetry centre. When the molecular point group become C_{4v}, the B_{1g} modes are still not symmetric with respect to the main axis, but they are symmetric with respect to the vertical symmetry plane, therefore they acquire the B_1 symbol. In the C_{2v} point group there is only a twofold symmetry axis and the B_{1g} vibrations are symmetric with respect to it; they also remain symmetric with respect to the vertical plane. Consequently, the B_{1g} vibrations acquire the A_1 symbol in the C_{2v} group. Using a similar procedure we can find all symmetry symbols corresponding to the ZnPc vibrations under C_{4v}, C_{2v} and C_s groups; further, we can examine which vibrations are Raman active in a similar way to that for the D_{4h} group. The results are collected in Table 2. To simplify further discussion we will use the symbols related to the D_{4h} group in the whole discussion.

Table 2
Symm. of Raman-active vibrations under various molecular symmetry point groups

D_{4h}	A_{1g}	A_{2g}	B_{1g}	B_{2g}	E_g	A_{1u}	A_{2u}	B_{1u}	B_{2u}	E_u
Out of resonance	a	n	a	a	a	n	n	n	n	n
Resonance Raman spectrum	a	a	a	a	n	n	n	n	n	n
C_{4v}	A_1	A_2	B_1	B_2	E	A_2	A_1	B_2	B_1	E
Out of resonance	a	n	a	a	a	n	a	a	a	a
Resonance Raman spectrum	a	a	a	a	n	a	a	a	a	n
C_{2v}	A_1	A_2	A_1	A_2	B_1/B_2	A_2	A_1	A_2	A_1	B_1/B_2
Out of resonance	a	a	a	a	a/a	a	a	a	a	a/a
Resonance Raman spectrum	a	a	a	a	n/n	a	a	a	a	n/n
C_s	A'	A'	A'	A'	A''	A''	A''	A''	A''	A'
Out of resonance	a	a	a	a	a	a	a	a	a	a
Resonance Raman spectrum	a	a	a	a	n	n	n	n	n	a

Symbols: a = active vibrations; n = non active vibrations.

The spectral characteristics of oxidized and reduced films are collected in Table 3. The band assignment is based on the normal mode calculation performed recently [4,16]. The normal mode assignment was based on the MNDO calculation results. The MNDO frequencies for the ZnPc molecule do not depart notably from those obtained by other normal mode treatments [31–36]. The difference between observed and calculated frequencies for Raman-active modes lies in the range 0–50 cm^{-1}. We have assumed that the error for the remaining bands is of a similar order.

The normal modes of phthalocyanine are delocalized over many internal coordinates, therefore only a brief description is given in Table 3. Bands that were observed in the Raman spectra of other ZnPc samples [16] are similarly assigned. For bands which change after oxidation of the ZnPc film all calculated frequencies are listed. The most characteristic feature of spectra of the oxidized ZnPc layer excited with both red and green radiation is the strong band appearing at 1600 cm^{-1}. The normal mode calculation yields three frequencies in the range between 1550 and 1650 cm^{-1}. These frequencies correspond to B_{2g} (ν_{39}), A_{2g} (ν_{65}) and E_u (ν_{96}) vibrations (the numbers of vibrations are the same as reported previously [16]. Since the 1600 cm^{-1} band does not appear in the spectra of the reduced film recorded with either green or red radiation, it is possibly forbidden in both normal and resonance Raman spectra under the D_{4h} molecular point group and it becomes allowed when the symmetry lowers. From Table 2 it follows that E_u vibrations fulfil this condition, when we assume that after oxidation the

Table 3
Bands observed in Raman spectra of ZnPc layers

Band positions/cm^{-1}				Assignments
Exc. 514.5 nm		Exc. 660 nm		
Red.	Ox.	Red.	Ox.	
226	226			ν_{30} B_{2g}: internal 16-memb. ring
		215	215	ν_{56} A_{2g}: H–C–C, C–N–Zn; ν_{45} E_g: benz. and N_β out-of-plane
254	248	248	248	ν_1 A_{1g}: isoindole in-phase motion; ν_{78} E_u: Zn–N, C–N–Zn, N–Zn–N; ν_{71} A_{2u}: N_α, benz. out-of-plane
283	272	283	283	ν_{46} E_g: N_α, N_β out-of-plane; ν_{119} B_{2u}: N_α, N_β and benz. out-of-plane
		480	480	ν_{31} B_{2g}: H–C–C, C–C–N pyrrole; ν_{48} E_g: benz. and N_β out-of-plane
	547		550	ν_{57} A_{2g}: C–C–C benz., C–C–N pyr.; ν_{106} A_{1u}: C benz., C pyr. out-of-plane
	567			ν_{49} E_g: C pyr., N_β out-of-plane; ν_{81} E_u: C–C–C benz.
590	590	590	590	ν_{16} B_{1g}: C–C–C benz., H–C–C; ν_2 A_{1g}: C–C–C benz., H–C–C, Zn–N
	633	640	640	ν_{58} A_{2g}: pyr. bending, H–C–C; ν_{82} E_u: C–C–C benz., Zn–N, C–C–N pyr., C–N–Zn
679	679	679	679	ν_3 A_{1g}: C–N_β–C; ν_{32} B_{2g}: C–C–C benz., H–C–C, H–C
746	746	746	746	ν_{17} B_{1g}: internal ring bending, Zn–N; ν_{50} E_g: pyr. out-of-plane def.
839wd		829wd		ν_{51} E_g: C pyr. out-of-plane; ν_{52} E_g: H, C benz. out-of-plane
	883			ν_{84} E_u: C–C–C benz., H–C–C, C–N–Zn, N–C–N; ν_{59} A_{2g}: C–C–C benz., H–C–C
945wd	945wd	945wd		ν_4 A_{1g}: Zn–N, C–N_α–C, C–N_β–C, C–C–C, C–C benz.; ν_{18} B_{1g}: C–C–C benz., C–C pyr., H–C, C–C benz.; ν_{33} B_{2g}: C–C–C benz., N–C–N, C–N–Zn
1008wd	1008wd		1008wd	ν_{53} E_g: benz. out-of-plane def.; ν_{108} A_{1u}: benz. out-of-plane def.
1035wd				ν_{54} E_g: H–C out of plane
1107		1107		ν_{34} B_{2g}: benz. in-plane def., N–C–N, C–N–Zn
	1123		1123	ν_{19} B_{1g}: H–C, C–C–C, C–C, H–C–C benz.; ν_{86} E_u: C–C–C, C–N–Zn
1145		1145	1145	ν_3 A_{1g}: C–C–C benz., H–C–C, H–C
	1180		1180	ν_6 A_{1g}: C–C benz., H–C–C; ν_{20} B_{1g}: C–C benz., H–C–C; ν_{60} A_{2g}: C–C–C benz., C–C pyr.; ν_{87} E_u: C–C–C benz., C–C benz., H–C
		1217	1217	ν_{35} B_{2g}: H–C–C, C–C benz, C–C–C benz., C–N_α, C–N–Zn
		1306	1306	ν_7 A_{1g}: H–C–C, C–C benz., C–N–Zn; ν_{21} B_{1g}: C–C benz., H–C–C
1340	1340			ν_8 A_{1g}: C–C benz., pyr. stretch.; ν_{36} B_{2g}: H–C–C; ν_{62} A_{2g}: H–C–C, C–N, C–N–Zn; ν_{91} E_u: H–C–C, C–C benz.; ν_{92} E_u: H–C–C, C–C benz., C–C pyr., C–C–N pyr., C–C–C benz.
1417	1417			ν_{22} B_{1g}: H–C–C, C–C benz., C–C pyr., C–N_α, C–C–C benz.
1430	1430			ν_{37} B_{2g}: C–N_α, H–C–C, C–C pyr., N–Zn–N; ν_{63} A_{2g}: H–C–C, C–N_α, C–N–Zn
1450		1450		ν_{23} B_{1g}: C–N_α, N–C–N, C–N–Zn, C–C pyr., N–Zn
1510	1510	1510	1510	ν_9 A_{1g}: H–C–C, C–C–C benz., C–C benz.; ν_{24} B_{1g}: H–C–C, C–C–C benz., C–C pyr., C–C–N pyr.
1546			1546	ν_{38} B_{2g}: C–C benz., H–C–C, C–C pyr., C–N; ν_{95} E_u: H–C–C, C–C benz., C–C pyr., C–C–C benz.; ν_{64} A_{2g}: C–C benz., H–C–C
1600	1600		1600	ν_{65} A_{2g}: N_β–C, C–C–N pyr., N–C–N, C–C pyr.; ν_{96} E_u: H–C–C, C–C benz., C–C pyr.; ν_{39} B_{2g}: C–C–N pyr., C–N_α, C–N–Zn, N_β–C

Symmetry symbols correspond to D_{4h} molecular symmetry; N_α = pyrrole nitrogen; N_β = bridge nitrogen; wd = wide band.

molecular point group is C_s. Because the A_{2g} vibrations are allowed only in the resonance spectrum (in the D_{4h} group), they should appear in the spectrum of neutral ZnPc excited with red radiation (Fig. 10(a) and (f)). However, we cannot exclude the possibility that the 1600 cm^{-1} band corresponds to the A_{2g} vibration, since A_{2g} vibrations have a strictly antisymmetric scattering tensor in the D_{4h} group [37] and they acquire significant Raman intensity only when the excitation wavelength lies between the $Q_{(0,0)}$ and $Q_{(0,1)}$ transitions [27]. In C_{2v} and C_s groups the A_{2g} vibrations also have the symmetric part of the scattering tensor and they can be observed irrespective of the excitation radiation wavelength. There are therefore two possibilities for the assignment of the 1600 cm^{-1} band (ν_{96} E_u or ν_{65} A_{2g}). The E_u vibrations are allowed in the C_s group. Assumption of C_s symmetry implies that all new bands (characteristic for the oxidized ZnPc) have E_u symmetry (Table 2), which roughly agrees with the list of frequencies given in Table 3; however, one can find also A_{2g} and A_{1u} vibrations near the new bands. The appearance of A_{2g} and A_{1u} would point rather to C_{2v} symmetry.

Another expected consequence of the C_s group is the vanishing of E_g modes in the spectrum in Fig. 11(b) (see Table 2). These modes are observed in the spectrum of the neutral ZnPc at 839, 1008 and 1035 cm^{-1} (Fig. 11(a)). Only the last one vanishes completely after oxidation of the film. The band at 1008 cm^{-1} even increases its intensity. However, in the C_{2v} group the E_g vibrations should also vanish in the resonance spectrum, and the increase of intensity of the 1008 cm^{-1} band can be explained when we assign the 1008 cm^{-1} band to the ν_{109} (A_{1u}) vibration. Therefore, the C_{2v} group after oxidation is more likely than C_s. The C_{2v} group matches the out-of-plane deformed structure of the ZnPc molecule.

Such a structure corresponds with the dimers of the ZnPc–ClO_4^- units, which were proposed in the discussion of the electroreflection results (Fig. 13(b)). In these units perchlorate anions are axially attached to the ZnPc macrocyclic dimer. In this situation the observed out-of-plane deformation of the ZnPc subunit agrees with the calculated results.

5. Conclusions

The anodic oxidation of ZnPc film is accompanied by inclusion of electrolyte anions. Large ions (such as benzenesulphonate) or with large hydration spheres (such as SO_4^{2-}) do not enter the layer. This observation agrees with results of Green and Faulkner [14] and Kahl et al. [17].

The anions occupy axial coordination sites of Pc molecules. This axial coordination causes a significant out-of-plane deformation of the ZnPc molecule. The deformation affects both ER and Raman spectra.

Because binding of the axial ligand follows the electrochemical oxidation of ZnPc, two processes contribute to the ER signal and as a result an unusual phase behaviour of ER spectra is observed.

The oxidation of the ZnPc film influences the Raman spectrum by a change of the resonance condition, which among other effects alters the relative band intensities. Bonding of anions to the axial site lowers the ZnPc molecular symmetry. The change of the molecular symmetry in turn affects the selection rules. In consequence, new bands appear in the spectrum. The detailed analysis of Raman bands reveals that the ZnPc molecule acquires C_{2v} symmetry (out-of-plane deformation and loss of the fourfold symmetry axis) in the oxidized film saturated with anions.

According to the MNDO calculation results, out-of-plane distortion is possible when only one axial site is occupied. Consequently, the final structure of the oxidized ZnPc film contains five-coordinated ZnPc-ClO_4 units. As the ZnPc to ClO_4^- ratio is unity, these units must form dimers as shown in Fig. 13(b).

Acknowledgments

The authors thank Dr. M. Savy (LCEMI, Université de Versailles) for stimulating discussions. They are also grateful to Mr. G. Scarbeck of the same institute for the preparation of the ZnPc samples.

References

[1] S. Srinivasan, J. Electrochem. Soc., 136 (1989) 41C.
[2] A. Billoul, F. Coowar, O. Contamin, G. Scarbeck, M. Savy, D. van den Ham, J. Riga and J.J. Verbist, J. Electroanal. Chem., 289 (1990) 189.
[3] F. Coowar, O. Contamin, M. Savy, G. Scarbeck, D. van den Ham, J. Riga and J.J. Verbist, J. Electroanal. Chem., 282 (1990) 141.
[4] B.J. Palys, Thesis, University of Twente, 1993.
[5] M. Savy, P. Andro, C. Bernard and G. Magner, Electrochim. Acta, 18 (1973) 191.
[6] H. Alt, H. Binder and G. Sandstede, J. Catal., 28 (1973) 8.
[7] D. van den Ham, C. Hinnen, G. Magner and M. Savy, J. Phys. Chem., 91 (1987) 4743.
[8] F. Coowar, M. Savy, G. Scarbeck, D. van den Ham, J. Riga, J. Riga and J.J. Verbist, J. Electroanal. Chem., 259 (1989) 241.
[9] J.A.R. van Veen and H.A. Colijn, Ber. Bunsenges. Phys. Chem., 85 (1981) 700.
[10] P.O. Carro, in K.M. Smith (Ed.) Porphyrins and Metalloporphyrins, Elsevier, Amsterdam, 1975, p. 123.
[11] B.D. Berezin and G.V. Semukowa, Kinet. Katal., 9 (1968) 528.
[12] I. Madi and A. Bolyos, Radiochem. Radioanal. Lett., 20 (1975) 215.
[13] I. Madi, Inorg. Nucl. Chem. Lett., 9 (1973) 767.
[14] J.M. Green and L.R. Faulkner, J. Am. Chem. Soc., 10 (1983) 3950.

[15] B.J. Palys, G.J. Puppels, D. van den Ham and D. Feil, J. Electroanal. Chem., 326 (1992) 105.
[16] B.J. Palys, D.M.W. van den Ham, W. Briels and D. Feil, J. Raman Spectrosc., submitted for publication.
[17] J.L. Kahl, L.R. Faulkner, K. Dwarakanath and H. Tachikawa, J. Am. Chem. Soc., 108 (1986) 5434.
[18] J.P. Dalbera, C. Hinnen and A. Rousseau, J. Phys. (Paris), Colloq., 38 (1977) C5-185.
[19] G.J. Puppels, F.F.M. de Mul, C. Otto, J. Greve, M. Robert-Nicoud, D.J. Arndt-Jovin and T.M. Jovin, Nature (London), 347 (1990) 301.
[20] G.J. Puppels, W. Colier, J.H.F. Olminkhof, C. Otto, F.F.M. de Mul and J. Greve, J. Raman Spectrosc., 22 (1991) 217.
[21] Convex Computer Corp., VAMP4.3 — vectorized AMPAC, QCPE, Program 506.
[22] J.C. Buchholz and G.A. Samorjai, J. Chem. Phys., 66 (1977) 573.
[23] J.F. Myers, G.W. Ryner Canham and A.B.P. Lever, Inorg. Chem., 14 (1975) 461.
[24] P.C. Minor, M. Gouterman and A.B.P. Lever, Inorg. Chem., 24 (1985) 1984.
[25] F.A. Cotton, in Chemical Applications of Group Theory, Wiley-Interscience, New York, 1970 pp. 316–320, 359.
[26] D. Dolphin (ed.), The Porphyrins, Vol. III, Physical Chemistry, Part A, Academic Press, New York, 1978.
[27] H. Hamaguchi, in R.J.H. Clark and R.E. Hester, (Eds.) Advances in Infrared and Raman Spectroscopy, Vol. 12, Wiley–Heyden, Chichester, 1985, 273–310.
[28] T.G. Spiro and T.C. Strekas, J. Am. Chem. Soc., 96 (1974) 338.
[29] A.J. Bovill, A.A. McConnell, B.N. Rospendowski and E. Smith, J. Chem. Soc., Faraday Trans., 88 (1992) 455.
[30] M.Z. Zgierski and M. Pawlikowski, Chem. Phys., 65 (1982) 335.
[31] R. Aroca, D.P. DiLella and R.O. Loutfy, J. Phys. Chem. Solids, 43 (1982) 707.
[32] C. Jennings, R. Aroca, A.-M. Hor and R.O. Loutfy, J. Raman Spectrosc., 15 (1984) 34.
[33] A.J. Bovill, A.A. McConnel, J.A. Nimmo and W.E. Smith, J. Phys. Chem., 90 (1986) 569.
[34] C.R. Bartholomew, A.A. McConnell and W.E. Smith, J. Raman Spectrosc., 20 (1989) 595.
[35] R. Aroca, Z.Q. Zeng and J. Mink, J. Phys. Chem. Solids, 51 (1990) 135.
[36] C.A. Melendres and V.A. Maroni, J. Raman Spectrosc., 15 (1984) 319.
[37] W.M. McClain, J. Chem. Phys., 55 (1971) 2789.